SPACE-TIME CORRELATIONS IN SEPARATED FLOW BEHIND A SURFACE MOUNTED OBSTACLE

Bård Venås and Lars R. Sætran
Department of Mechanics, Thermo and Fluid Dynamics
Norwegian University of Science and Technology
N-7034 Trondheim, Norway

ABSTRACT

Autocorrelations and two-point correlations are reported from separated flow behind a surface mounted triangular cylinder, using both pulsed and conventional hot-wire anemometry. Autocorrelations and spectra reveal separate large scales throughout the flow, notably, scales owing to vortex shedding from the separation and very low frequency fluctuations. Two-point correlations indicate considerable correlation between the backflow and the outer flow. Both vortex shedding and large-scale fluctuations are detected in these measurements, indicating that these features affect the whole of the flow.

INTRODUCTION

In this paper we study the flow past a sharp edged surface mounted obstacle with very thin inflow boundary layers. The motivation for the work was trying to better understand the turbulence structure of massively separated flow zones. The triangular cylinder experiment recently published by Heist and Gouldin (1997) (later referred to as HG) was chosen since it is well defined and well suited for one of the wind tunnels in our laboratory, and since new high quality data were available for comparison. Numerical calculations have also been published for the experiment (Heist et al., 1994).

The main focus in the paper of Heist and Gouldin is Reynolds averaged quantities. We wanted to look into the temporal and spatial structure of the flow, including the highly turbulent separated region, where such information is rare. Features under investigation were reported periodicities in separated flows; a low frequency 'oscillation' have been found in the outer shear layer, and at frequencies much lower than those characterized by the vortex shedding in the separated shear layer (similar to the mixing layer; see e.g. HG for references). We further wanted to try finding whether, or how, this behavior was linked to large-scale motions in the backflow region.

To provide information on spatial relationships in the separated zone one has to resort to multi-point measurements since Taylor's frozen turbulence hypothesis breaks down for high turbulence intensities. Some full flow field experiments in separated flows have been reported using Particle Image Veliocimetry; e.g. Grant et al. (1992). The state of the art of this approach, however, seems to be that it is currently difficult to use PIV to derive quantitative information of the type we were seeking, that is, turbulence spatial correlations and spectra. This is due to technical limitations in factors such as: spatial resolution, picture size and (time) sampling frequency, in the case of digital PIV, and for photographic PIV as well, the number of samples practically obtainable.

The only two-point correlation measurements in(side) separated flows known to the authors are the experiments of Nasser and Castro (1989) using pulsed wire anemometry in the much tested 'bluff plate with splitter plate' flow, and spanwise correlations from the backward-facing step flow of Eaton and Johnston (1980). The paper of Nasser and Castro, however, tends more toward technology demonstration than flow analysis and the number of measurements and physical interpretation of the results are relatively scarce. Eaton and Johnston presents data using pairs of thermal tufts deep in the separated flow, estimating correlations from these data.

Other researchers have published two-point correlations with slightly different focus: Gould and Benedict (1994) conducted laser doppler two-point measurements in a sudden expansion flow, but outside the separated zone. Driver et al. (1987) present two-point hot-wire measurements behind the reattachment of the backward facing step flow. Further, a couple of papers provide velocity vs. wall pressure and two-point wall pressure correlations from the 'blunt leading edge' separation (Kiya and Sasaki, 1983; Cherry et al., 1984).

In spite of these experiments, the conclusion after searching the litterature, is that little is known about the turbulence structure of separated flows. A reason for this may be that that the most natural choice of measuring technique, Laser Doppler Anemometry, probably will be difficult to use for this type of experiment, due to low particle arrival rates in highly turbulent flows. Low frequency and non-periodicity of the samples will make it difficult to obtain simultaneous samples from more than one measuring point, and thus to calculate correlations.

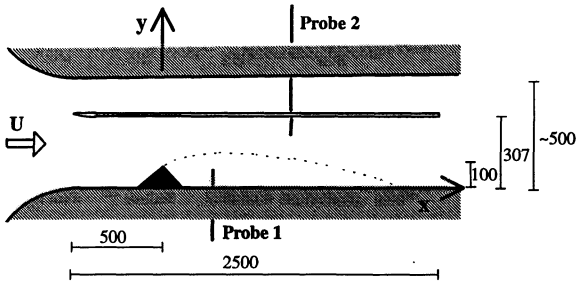

Figure 1. Sketch of wind tunnel configuration and coordinate system (measures in [mm]).

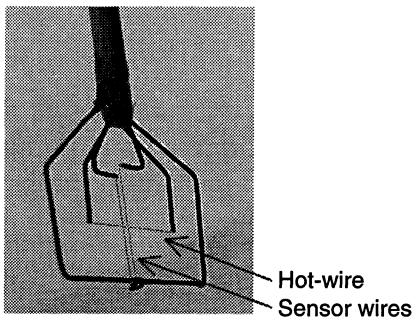

Figure 2. Pulsed hot-wire probe.

EXPERIMENTAL DETAILS

The experiment was performed in a 1m x 0.5m test section closed return wind tunnel. In order to obtain a higher obstruction width to height ratio a 2.5m long 15mm thick splitter plate was mounted in the test section, with its lowest surface 307mm above the test section floor. The leading edge of the plate was rounded elliptically to minimize flow disturbance. The wind tunnel roof was kept in its zero pressure gradient, weakly diverging configuration. From pitot-static tube measurements the flow below the plate was found to be homogeneous to within approximately 3% outside wall boundary layers.

The model has a height of 100mm and is geometrically similar to that in HG; measuring 153mm horizontally from leading edge to apex and 113mm from there to the trailing edge. It was mounted on the wind tunnel floor, 0.5m downstream of the splitter plate leading edge (Figure 1).

The reference velocity was measured using a pitot-static tube placed upstream of the splitter plate, shifted a distance away from the measuring plane (the central plane) to reduce any disturbance effects. The reference velocity U_{ref} used for non-dimensional values is the mean velocity midway between the model apex and the lower side of the plate. The ratio between this velocity and the one measured by the upstream pitot-static tube was calibrated prior to the experiments, using a pitot-static tube in each position. The reference velocity used was 4.2m/s, giving a mean flow Reynolds number ($U_{ref}H/\nu$) of $2.8 \cdot 10^4$, equal to that in HG.

Pulsed hot-wire anemometry (PHWA) was used in regions of the flow containing reverse flow. Conventional constant temperature hot-wire anemometry (CTA) was used in regions of lower turbulence intensity, where this technique is appropriate (turbulence intensities of, say, less than 30%).

Pulsed Hot-Wire Anemometry was first described by Bradbury and Castro (1971), as a means for measuring flows including both mean and intermittent backflow; notably turbulent separated flows. A picture of one of the probes used is shown in Figure 2. The wires are not visible in the original picture, but have added for illustration.

The PHWA working principle is that the anemometer circuitry 'fires' the central wire with a high current square wave, repeatedly, for short periods of time. This heats the wire to a temperature well above the ambient and thereby the adjacent fluid surrounding the wire. This fluid convects with the instantaneous flow and is detected a time later as a temperature rise by one of the sensor wires, which are operated as resistance thermometers. The anemometer measures the time-of-flight from emission to detection, and knowing the distances between the wires, the velocity can be calculated. However, since the distances are not known exactly, a velocity calibration is performed prior to measurements - relating the anemometer output voltages to the flow velocity. Sensor wires are placed both upstream and downstream of the pulsed wire to detect flow both in the forward and in the backward direction. The anemometers used for these tests are designed and manufactured at our department (Krogstad, 1991). For more details on pulsed hot- wire anemometry and references, see e.g. the review by Castro (1992), or the internal report covering the work reported here (Venås and Sætran, 1998).

The measurements were sampled using a standard PC equipped with a 12-bit A/D conversion board. The sampling rate is equal to the 'firing rate' of the pulsed wire, which was 50Hz. Between 10000 and 50000 samples where taken in each measuring point (numbers of samples are referred to in the text for the different measurements). The conventional hot-wire anemometry measurements were made using in-house built anemometers and standard DISA single-wire probes with 5 μm Tungsten wires.

In all one-point measurements, the probe was inserted into the flow from the upper side of the wind tunnel, through slots in the wind tunnel roof and in the splitter plate, running streamwise along the centerline of the tunnel (Figure 1). To avoid flow through the slots due to pressure differentials, the slots were sealed by heavy-duty tape after every x-direction adjustment of the probe. In two-point measurements the second probe (note, this is 'probe 1' in text and equations) was inserted from below, through a similar slot running along the wind tunnel floor. The probe position is measured relative to the horizontal/pulsed wire.

MEAN FLOW STRUCTURE

Figure 3a) shows mean velocity profiles at all the measuring positions along the flow, from 10000 sample PHWA measurements. The figure is scaled so that $\Delta x/H=1$ corresponds to $U/U_{ref}=1.5$. In the figure is also a line representing the 'separation zone' - determined as the position of zero volume flow when integrating the mean velocity profile upwards from the floor. We clearly see the

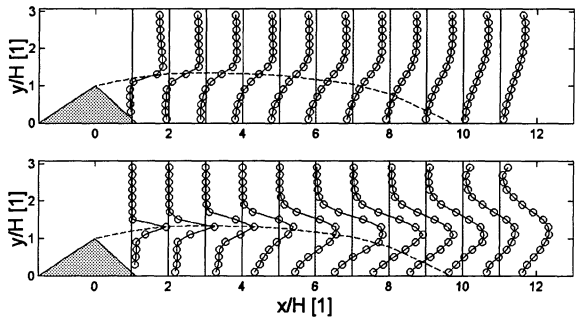

Figure 3. a) Mean velocity U/U_{ref}
b) Normal stress $\overline{uu}/U_{ref}^2$

typical features of this type of flow: a strong, gradually relaxing, velocity shear behind the separation point and a mean backflow close to the floor. There is an acceleration of the 'free stream' above the separation zone up to approximately x/H=3 and then deceleration. The mean reattachment length is found to be x=9.7H, from linear interpolation and extrapolation (down to y=0) of the mean velocity measurements. This is close to the value of 9.8H reported in the reference experiment. The turbulence normal stress $\overline{uu}/U_{ref}^2$ is plotted in Figure 3b), in a scale such that $\Delta x/H$=1 corresponds to $\overline{uu}/U_{ref}^2$=0.05. Main characteristics are that the turbulence level has a maximum value a bit above the apex, which increases downstream approximately to x/H=7, where it starts to decay.

SINGLE-POINT CORRELATIONS AND SPECTRA

Spectra along x/H=2

Figure 4 shows turbulence spectra for different y-positions at x/H=2. This position is chosen as an example since many characteristics seen throughout the flow can be seen very clearly in this region. PHWA is used for measurements within the separated zone (y/H=0.1-0.9), while conventional hot-wire anemometry is employed for y/H=1.3 and upwards. The PHWA spectra are based on 50.000 samples each (the data set from the two-point measurements presented in the next section). The hot-wire spectra are based on 500.000 samples each, taken at a sampling rate of 500Hz.

The spectra at the positions y/H=0.1-0.9, i.e. inside the backflow region are close to equal both in shape and in energy level, and in the figure only the spectrum at y/H=0.5 has been plotted. The backflow spectra resembles typical one-dimensional turbulence spectra - apparently having a breaking frequency, defining the dominant large scale and what seems to be constant roll-off for higher frequencies. In the spectra from above the separation zone however, we see an emerging peak at a dimensionless frequency of ca. 0.3, and as the total energy drops with increasing y-value, this peak becomes more pronounced.

Some discrete noise peaks are seen in the measurements, first in the y/H=1.7 spectrum, becoming more numerous and significant with increasing y. The peaks are associated with

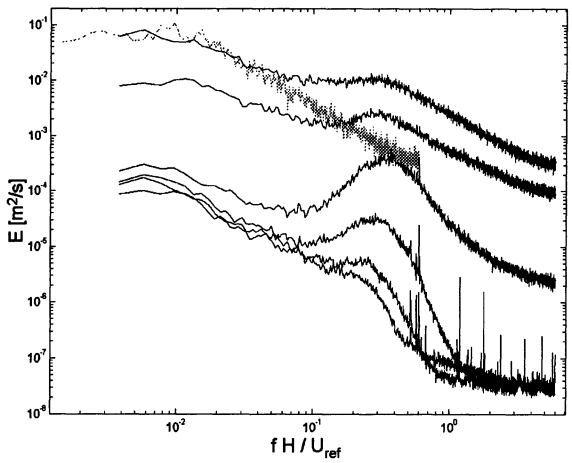

Figure 4. Spectra along x/H=2. From above, according to energy level, y/H=0.5 (gray), 1.3, 1.5, 1.7, 2.1, 2.5 and 2.9.

electric noise from the wind tunnel motor and are found at 25Hz and higher harmonics. However, the turbulence intensities for y/H=[1.7, 2.1, 2.5, 2.9] are respectively [2.2%, 0.68%, 0.61%, 0.45%] and the noise peaks are of little significance to the analysis. The hot-wire signal for zero velocity corresponded to under 0.1% turbulence intensity for these velocities, and it should be clear that these magnitudes are at the brink of the anemometer accuracy.

Characteristic features of the autocorrelation

Due to the somewhat low sampling frequency obtainable for the region of high turbulence intensity (where PHWA is needed) autocorrelations may provide just as good insight into the nature of the large-scale time/frequency characteristics, as spectra can. This, since the phenomena of aliasing and noise in spectra are difficult to analyze, if they are significant, and the autocorrelation presents just the same information, but in a sometimes more intuitive fashion.

Figure 5 shows three autocorrelation functions from the measurements at x/H=2. In the backflow region (y/H=0.5) the correlations fall off near exponentially, as usually found in turbulent flows. In the shear layer (y/H=1.3), a much faster decay at small time lags starts to emerge, signifying that smaller time scales start to dominate the flow. The curve here resembles the sum of two exponentially decaying functions, and this may be interpreted as that the initial decay represents a small time scale ($\Delta t U_{ref}/H$~0.5), and the persisting tail along the time axis another, much larger, scale ($\Delta t U_{ref}/H$~10). This idea of two separate scales has earlier been suggested by Castro (1985). Further we see that at y/H=1.3, there is a slight dip in the correlation near the break between the small and large-scale regions, and at y/H=2.1 this dip is very significant.

Both the dip and the large-scale correlation tail are found for most measurements, all the way up to the roof. These two features have clear parallels in the spectra of Figure 4; a strictly exponential decay corresponds to a spectrum with a

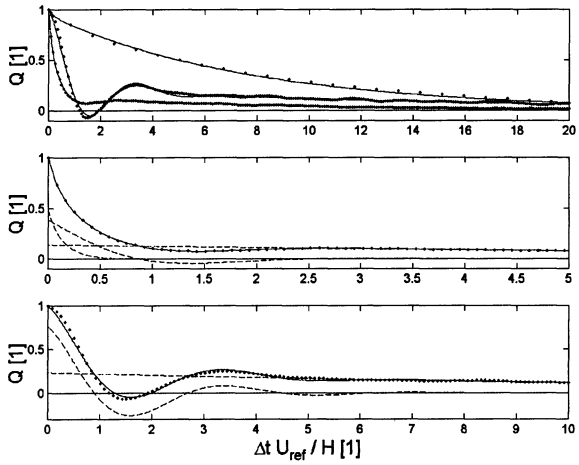

Figure 5. Autocorrelations at x/H=2. The dots are measured values, — total curve fit, and - - - individual curve fit terms.

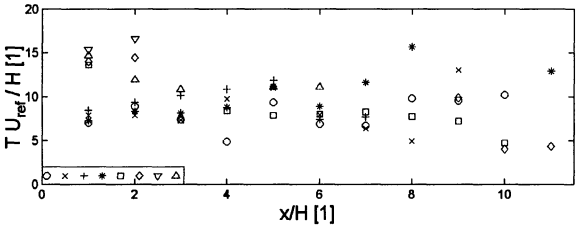

Figure 6. Large scale fluctuation, T_2 U_{ref}/H. Legend in lower left corner (y/H along x-axis).

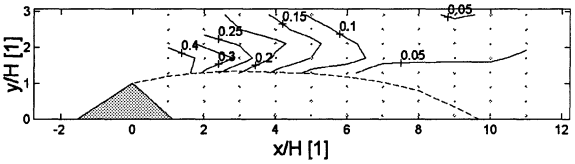

Figure 7. Oscillation frequency, f_{osc} H/ U_{ref}.

constant level at low frequencies and constant roll-off for high frequencies (E~f^{-2} for exponential decay, E~$f^{-5/3}$ for an 'inertial subrange'). At y/H=1.3 the emerging peak in the spectrum corresponds to the smaller time scale and the oscillation, while the low frequency 'shoulder' in the spectrum stems from the correlations at longer lag times.

To get a better picture of what these results represent we have tried to quantify the characteristics mentioned here. A strictly exponentially decaying correlation function is the Dryden (1943) model form: $Q(\Delta t)=e^{-\Delta t/T}$, where Δt is the time lag and T the integral time scale of turbulence. This is a relatively good approximation to the measurements in the near region behind the obstacle, such as at x/H=2, y/H=0.5.

The two-scale correlation can be fitted by superimposing two such exponential functions, representing the two scales through separate time constants. The dips in the correlations probably represent oscillations and the best equation found for this feature is to modulate the exponentially decaying curve with a cosine. In sum, this gives a three-term model of the form

$$Q(\Delta t)=c_1 e^{-\Delta t/T_1}+c_2 e^{-\Delta t/T_2}+(1-c_1-c_2)\cos(2\pi f_{osc}\Delta t)e^{-\Delta t/T_3} \quad (1)$$

where c_1 and c_2 are parameters valued between 0 and 1 as is their sum, signifying the relative importance of the terms. f_{osc} describes the location of the dip or the oscillation frequency, whereas T_1 and T_2 are measures for respectively the small and the large time scale. T_3 describes the decay, or the memory, of the oscillation. In Figure 5 three examples of curve fits are shown. At y/H=0.5 there is only the large-scale fluctuation, at y/H=2.1 there is large-scale fluctuation and oscillation, and at y/H=1.3 all three terms are needed to provide a good fit.

Although yielding good fits, the exact value of the large scale T_2 is rather uncertain in much of the flow, due to low correlation values compared to inherent 'ringing noise' in the experimental correlation estimates. In Figure 6 significant (threshold set at c_2>0.05) values for this time scale is shown. A typical dimensionless value of 10 is found throughout the flow; generally ranging roughly from 5 to 15. Figure 7 shows the oscillation through an iso-contour plot of the values for f_{osc}. The oscillation is found throughout most of the 'free stream' region, and also in the outer shear layer. The frequency is seen to decrease downstream, a phenomenon which has been contributed to the large scale structures growing downstream, in the same manner as in a free shear layer (Djilali and Gartshore, 1991).

TWO-POINT CORRELATIONS

Since the flow is highly inhomogeneous in the x-y-plane, two-point correlations R are presented as functions of both probe positions, (x_1, y_1) and (x_2, y_2), i.e.

$$R(x_1, y_1, x_2, y_2, \Delta t) = \overline{u(x_1, y_1, t)\, u(x_2, y_2, t+\Delta t)} \quad (2)$$

where overline represents the time mean value. Correlation coefficients Q are normalized in the standard manner, by the fluctuation intensities at both probes.

To search for couplings between the backflow region and the rest of the flow, two-point measurements were conducted with probe 1 stationary in the position, x/H=6, y/H=0.1. This is as close to the wall (y=10mm) as is possible with the probe utilized here, meaning that only the prongs are above the wind tunnel floor. Probe 2 was traversed in a grid comprising of 11 x-positions and 8 y-positions ($\Delta y/H$=0.1-2.9 in steps of $\Delta y/H$=0.4). 50000 samples were taken in each measurement in order to get good statistical accuracy even for low absolute correlation values. From position y/H=1.7 and above, conventional hot-wire anemometry was used for probe 2 measurements.

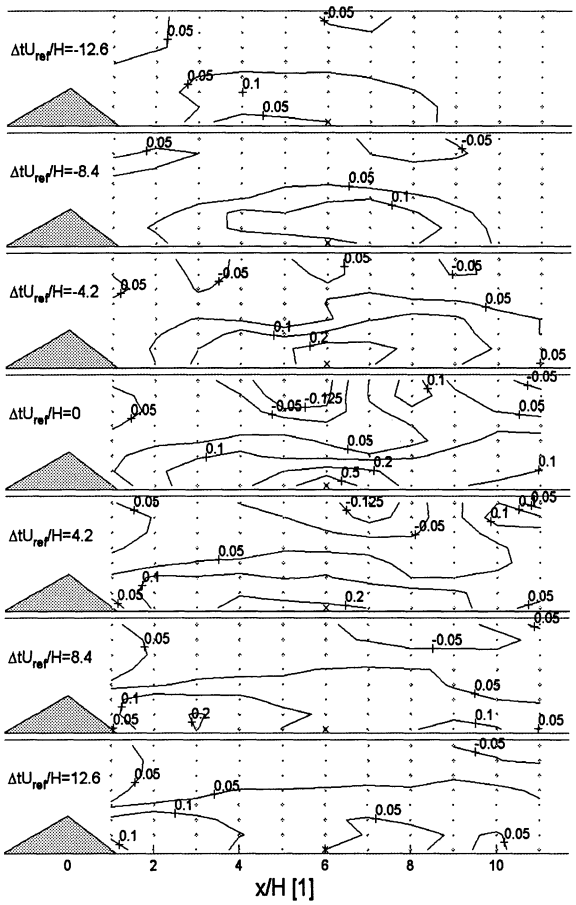

Figure 8. Two-point correlations, *x/H=6, y/H=0.1.*

Figure 8 shows iso-contours of Q for seven different time lags. Looking at the zero time lag case, one may conclude that the length scale is close to equal to H in the x-direction, and a little less than half this value in the y-direction. This is based on a typically correlation value for the time scale, being $Q \approx 0.3$ for an exponentially decaying correlation. One further notices quite significant negative correlation along the roof; having one center at $x/H \approx 5$ and possibly another somewhere aft of $x/H \approx 11$, with a positive region in-between.

The negative correlations indicate that there is a tendency (i.e. in the mean) for the upper flow to fluctuate in the opposite direction of the flow near the floor. The correlation says nothing about the mechanism behind this, but remembering the normalization - the value of the correlation is quite low compared to the fluctuations in the backflow, but high compared to the fluctuations near the roof. Reasoning around this, the magnitude of an effect of the outer flow (e.g. the vortex shedding) on the inner flow is rather low. On the other hand, the coupling is very significant for the upper flow. This may be, either or both, correlation between vortices shed in the separation process and the backflow region (strictly speaking: $x/H=6$, $y/H=0.1$), or that fluctuations in the backflow perturbs the outer flow.

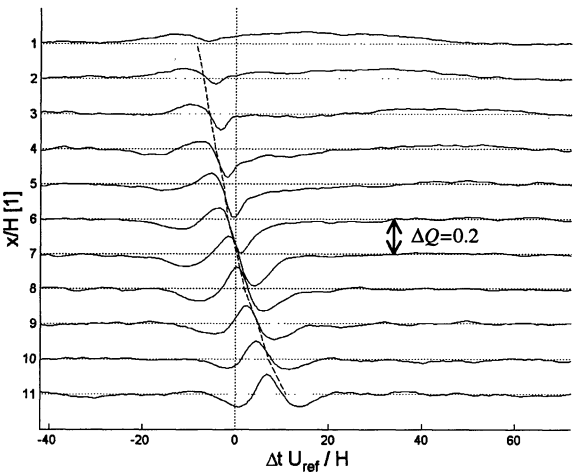

Figure 9. Two-point correlations along *y/H=2.9.*

In a 'convective flow' the locus of the correlation should move downstream with the local mean velocity. In the separated flow this can clearly not be seen for negative time lags: the correlation here seems to be quite low in value, widespread, stationary, and centered near the origin (by definition the case for $\Delta t=0$). For positive time lags a maximum correlation point moves with the mean velocity, that is to say, in the upstream direction. This locus, however, has a low value, meaning that it can not be said to be a convective motion - merely that there is a tendency for structures to move in this direction. Along the roof one can recognize the negative correlation regions mentioned earlier, moving downstream with time. The downstream locus is located above the lower wall probe for the first time lag, and leaves the measuring domain just after $\Delta t=0$. The second locus first appears at $x/H=3$ for $\Delta t/H=-4.2$, and moves to the end of the domain during the time span covered in the figure.

A better understanding of this structure can be provided by plotting the cross correlation as function of time, as is done in Figure 9 for the points along $y/H=2.9$. One can here see very large scale correlations at the forward-most measuring stations, which are the same as the constant 0.05 iso-contour in this region in Figure 8. From $x/H=1$, and all the way downstream, a dip is found in the correlation, which grows somewhat larger and moves along the time axis for downstream measurements. The dashed line in the figure corresponds to a convection velocity 0.6 times the local mean velocity. A vortex convection velocity like this is similar to what is reported for the backward facing step, where it is stated to be 0.6 times the *upstream* free stream velocity (Troutt et al., 1984; Simpson, 1989).

The fact that the vortices, and the convection of them, are identified by two-point measurements, means that the same vortex system influences both the fluctuations along the roof and the backflow. The oscillations in the outer flow should be evident from Figures 4 and 5, showing periodicity, based on the one-point measurements. However, oscillations are not identified from one-point measurements in the backflow, probably since the effect is small compared to the general fluctuation level here.

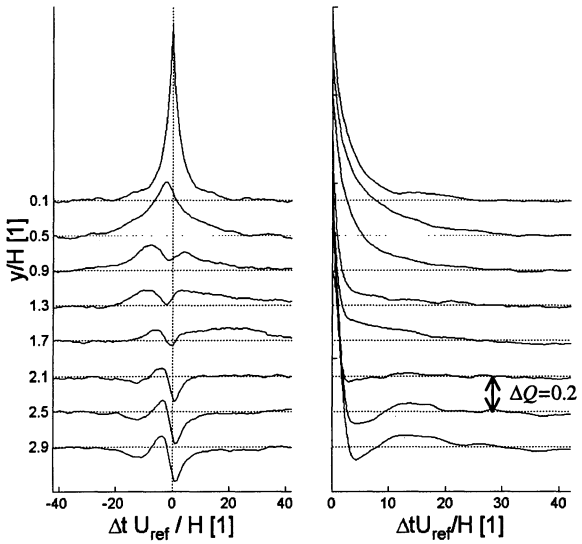

Figure 10. a) Two-point correlations, and b) autocorrelations along x/H=6.

This can be studied more closely in Figure 10, where two-point and autocorrelations are plotted beside each other, along x/H=6. The oscillations are visible from y/H=0.9 in the two-point correlation, but not for the lower positions. It seems as that the correlation is a summation of a general exponentially decaying fluctuation, and an (wave-like) oscillation.

In the autocorrelations oscillations are seen only for the highest y-positions, while correlations at large time scales are found in both types of measurements. It is noticed that the large-scale fluctuations at this x-position (generally the latter part of the separation zone) are comparable with the oscillations, in frequency. This oscillation frequency, found towards the reattachment position is close to values reported from other separated flows, e.g. (Driver et al., 1987) and (Cherry et al. 1984), reporting values of ca. 0.06-0.07.

CONCLUSIONS

Oscillations (partially periodic) and large time scale fluctuations (non-periodic) have been identified from one- and two-point measurements. Vortices shed in the separation process are found to influence the whole flow downstream. The mechanisms behind the large scale fluctuations are unclear, but may be linked to coupling with the oscillations in the latter part of the separation zone (comparable in frequency) or perturbation from fluctuations in the separated flow zone (comparable in time scale).

ACKNOWLEDGEMENT

The authors would like to express their sincere gratitude to Professor Per-Åge Krogstad for his essential help with the pulsed hot-wire technique.

REFERENCES

Bradbury, L. J. S., and Castro, I. P., 1971, "A Pulsed-Wire Technique for Velocity Measurements in Highly Turbulent Flows," *Journal of Fluid Mechanics*, Vol. 49, pp. 657-691

Castro, I. P., "Pulsed-Wire Anemometry, 1992, " *Experimental Thermal and Fluid Science*, Vol. 5, pp. 770-780

Castro, I. P., 1985, "Time-Domain Measurements in Separated Flows," *Journal of Fluid Mechanics*, Vol. 150, pp. 183-201

Cherry, N. J., Hillier, R., and Latour, M. E. M. P., 1984, "Unsteady Measurements in a Separated and Reattaching Flow," *Journal of Fluid Mechanics*, Vol. 144, pp. 13-46

Djilali, N., and Gartshore, I. S., 1991, "Turbulent Flow Around a Bluff Rectangular Plate. Part 1: Experimental Investigation," *Journal of Fluids Engineering*, Vol. 113, pp. 51-59

Driver, D. M., Seegmiller, H. L., and Marvin, J. G., 1987, "Time-Dependent Behavior of a Reattaching Shear Layer," *AIAA Journal*, Vol. 25, No. 7, pp. 914-919

Eaton, J. K., and Johnston, 1980, "Turbulent Flow Reattachment: An Experimental Study of the Flow and Structure Behind a Backward-Facing Step," Report MD-39, Thermosciences Division, Department of Mechanical Engineering, Stanford University

Gould, R. D., and Benedict, L. H., 1994, "Comparison of Length Scale Estimates for a Sudden Expansion Flow Estimated from Spatial and Autocorrelation LDV Measurements," *Experiments in Fluids*, Vol. 7, pp. 119-124

Grant, I., Owens, E., and Yan, Y.-Y., 1992, "Particle Image Veliocimetry Measurements of the Separated Flow Behind a Rearward Facing Step," *Experiments in Fluids*, Vol. 12, No. 4/5, pp.238-244

Heist, D. K., Ravichandran, M., and Gouldin, F. C., 1994, "Incinerator Related Flows: An Experimental and Numerical Study of Turbulent Flow over an Obstacle," *Combustion Science and Technology*, Vol. 101, pp. 425-441

Heist, D. K., and Gouldin, F. C., 1997, "Turbulent Flow Normal to a Triangular Cylinder," *Journal of Fluid Mechanics*, Vol. 331, pp. 107-125

Kiya, M., and Sasaki, M., 1983, "Structure of a Turbulent Separation Bubble," *Journal of Fluid Mechanics*, Vol. 137, pp. 83-113

Krogstad, P.-Å., 1991, "Pulsed Hot Wire and Constant Temperature Anemometer –User Manual and Specifications, Division of Hydro and Gas Dynamics, Norwegian Institute of Technology

Nasser, S. H., and Castro, I. P., 1989, "Spatial Correlation Measurements in Turbulent Flows Using Pulsed Wire Anemometry", *Experiments in Fluids*, Vol. 7, pp. 119-124

Simpson, R. L., 1989, "Turbulent Boundary-Layer Separation," *Annual Review of Fluid Mechanics*, Vol. 21, pp. 205-234

Troutt, T. R., Scheelke, B., and Norman, T. R., 1984, "Organized Structures in a Reattaching Separated Flow Field," *Journal of Fluid Mechanics*, Vol. 143, pp. 413-427

Venås, B., and Sætran, L. R., 1998, "Space-Time Correlations in Separated Flow Behind a Surface Mounted Obstacle," MTF-Report 1998:166(A), Norwegian University of Science and Technology